Electronic Supplementary Material (ESI) for ChemComm.
This journal is © The Royal Society of Chemistry 2021

Electronic Supplementary Information

A Cylinder-Shaped Macrocycle Formed via Friedel-Crafts Reaction

Dingsheng Zhu, Shuai Fang, Lu Tong, Ye Lei, Guangcheng Wu, Tayba Chudhary and Hao Li*

Department of Chemistry, Zhejiang University, Hangzhou 310027, P. R. China.
E-mail: lihao2015@zju.edu.cn

Table of content

1. Materials and general methods

All reagents and solvents were purchased from commercial sources and used without further purification. Manipulations were performed under a normal atmosphere unless otherwise indicated. The cage precursor 1,3,5-tri(furan-2-yl) benzene (**TFB**) was prepared according to reported procedure[s1]. Nuclear magnetic resonance (NMR) spectra were recorded at ambient temperature using Bruker AVANCE III 400/500 and Agilent DD2 600 spectrometers, with working frequencies of 400/500/600 and 100/125/150 MHz for ^{1}H and ^{13}C, respectively. Chemical shifts are reported in ppm relative to the residual internal non-deuterated solvent signals ($CDCl_3$: δ = 7.26 ppm). High-resolution mass spectra (HRMS) were recorded on a Fourier transform ion cyclotron resonance mass spectrometry (FT-ICR MS). X-ray crystallographic data were collected on a Bruker D8 Venture diffractometer.

2. Synthetic procedures

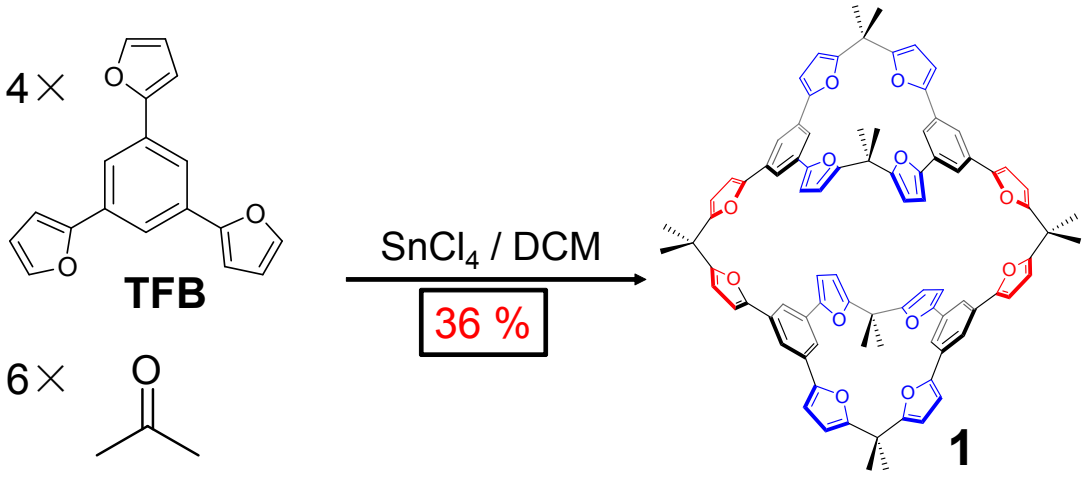

Figure S1. Synthesis of **1**

Synthesis of 1

1,3,5-tri(furan-2-yl) benzene (TFB) (200 mg, 0.72 mmol) and acetone (0.239 mL, 3.26 mmol) were dissolved in anhydrous dichloromethane (48 mL). $SnCl_4$ (0.256 mL, 2.17 mmol) was added slowly. The reaction mixture was stirred under the protection of a N_2 atmosphere at 298K. The progress of the reaction was monitored by TLC. After the reaction reached its equilibrium after 72 h, the reaction mixture was poured into cold water (100 mL), which was extracted with DCM (40 mL x 2). The organic layer was washed with saturated aqueous solution of $NaHCO_3$ (100 mL) and brine water (100 mL). After drying with Na_2SO_4, the solvent was removed under vacuum. The crude product was purified by column chromatography (silica gel: ethyl acetate/petroleum ether = 1:5) to obtain **1** as an off-white powder (87 mg, 36%). Rf = 0.76, ethyl acetate/petroleum ether = 1:3. Elem. anal. : observed: C 73.83% H 5.78%, calculated: C 80.34% H 5.19% .^{1}H NMR (600 MHz, $CDCl_3$): δ 8.13 (8.12 (t, *J* = 1.6 Hz, 4H)), 7.48 (d, *J* = 1.7 Hz, 8H), 6.57 (d, *J* = 3.3 Hz, 4H), 6.50 (d, *J* = 3.3 Hz, 8H), 6.23 (d, *J* = 3.4 Hz, 4H), 6.09 (d, *J* = 3.4 Hz, 8H), 1.89 (s, 12H), 1.77 (s, 12H), 1.73 (s, 12H). ^{13}C NMR ($CDCl_3$, 600 MHz): δ 160.1 (C), δ 159.9 (C), δ 158.8 (C), δ 152.3 (C), δ 132.0 (C), δ 131.5 (C), δ 117.0 (CH), 116.5 (CH), 106.2 (CH), 106.1 (CH), 106.0 (CH), 105.2 (CH), 37.7 (C), 37.1(C), 26.8 (CH_3), 26.2 (CH_3), 24.9 (CH_3). ESI-HRMS: $[M+H]^+$, obeserved: *m*/*z* 1345.5044, calculated: *m*/*z* 1345.5097; $[M+Na]^+$, oberved: *m*/*z* 1367.4838, calculated: *m*/*z* 1367.4916; $[M+K]^+$, oberved: *m*/*z* 1383.4545, calculated: *m*/*z* 1383.4655. IR: 3455.54 cm^{-1}, 2975.44 cm^{-1}, 2933.22 cm^{-1}, 1611.31 cm^{-1}, 1586.36 scm^{-1}, 1542.14 cm^{-1}, 1210.39 cm^{-1}, 1586.36 cm^{-1}, 1542.14 cm^{-1}, 1255.63 cm^{-1}, 1210.39 cm^{-1}, 1025.44 cm^{-1}, 781.67 cm^{-1}, 757.27 cm^{-1}.

3. Characterization

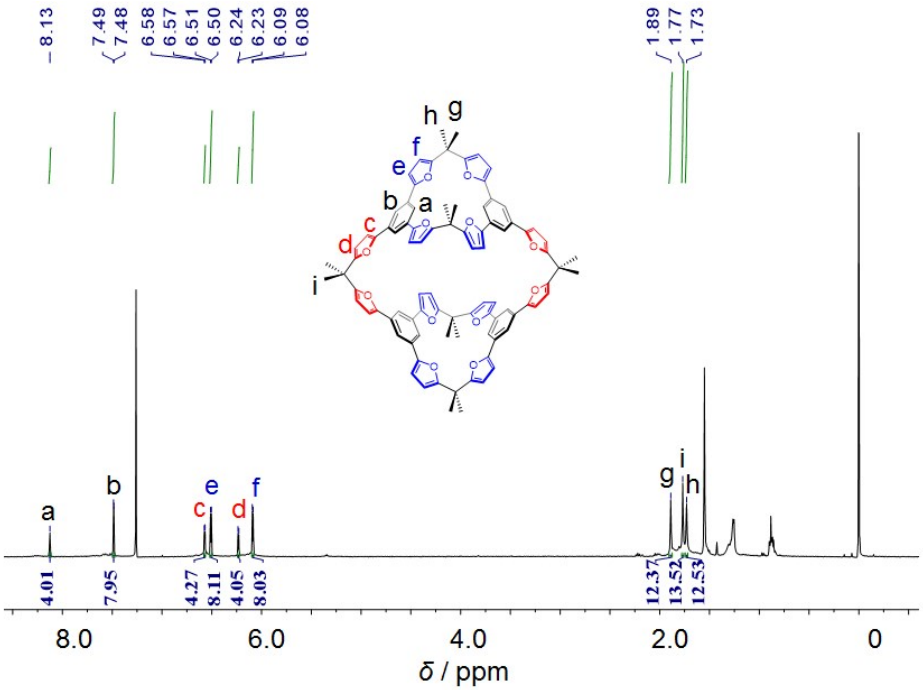

Figure S2.[1]H NMR spectrum of **1** ($CDCl_3$, 600 MHz, 298 K).

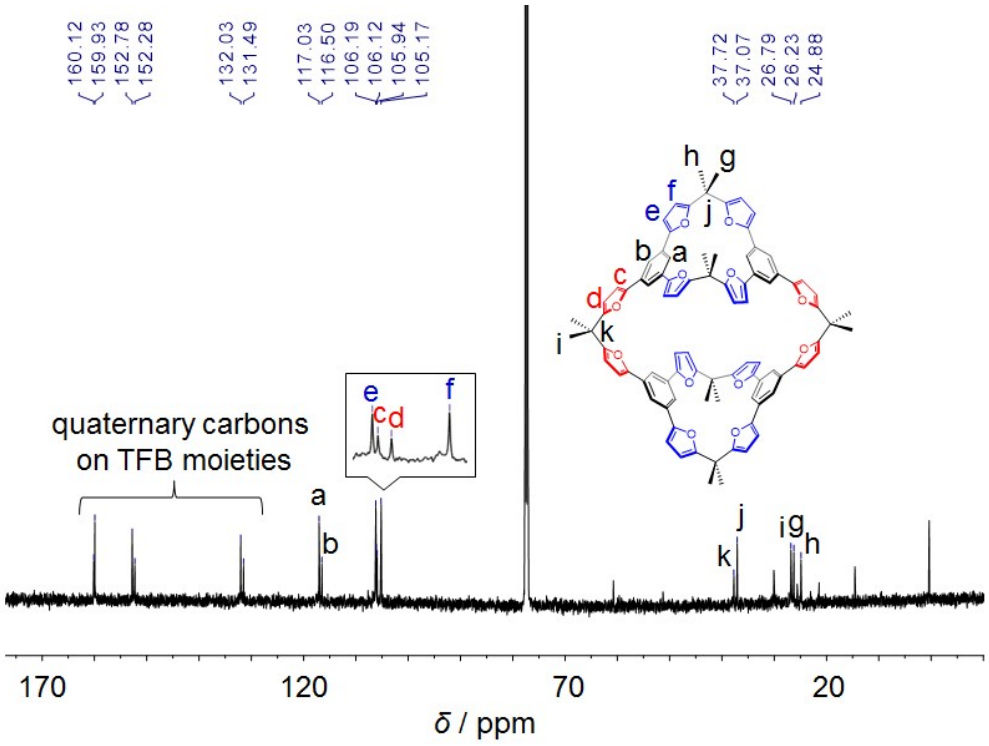

Figure S3.[13]C NMR spectrum of **1** ($CDCl_3$, 150 MHz, 298 K).

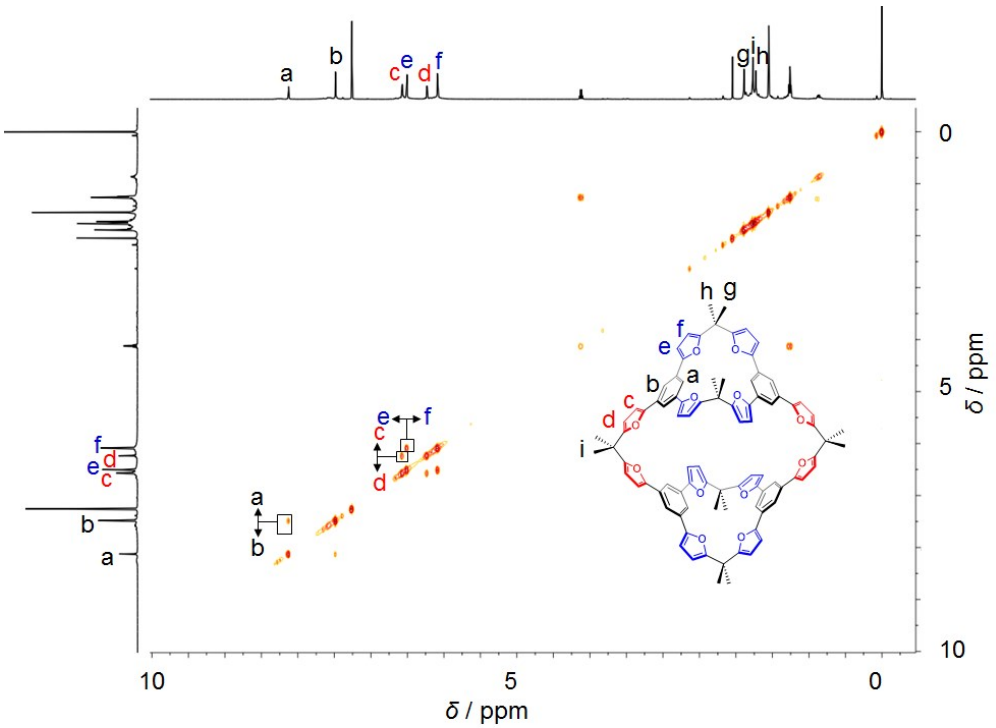

Figure S4. ^{1}H-^{1}H COSY NMR spectrum of **1** ($CDCl_3$, 500 MHz, 298 K). Key correlation peaks are labeled in the spectrum.

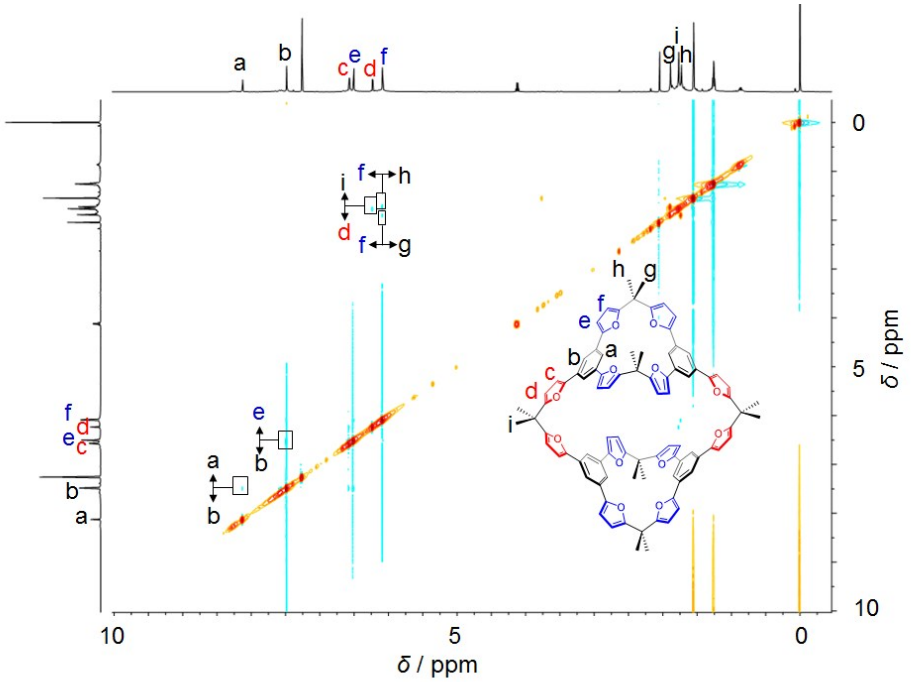

Figure S5. ^{1}H-^{1}H NOESY NMR spectrum of **1** ($CDCl_3$, 500 MHz, 298 K). Key correlation peaks are labeled in the spectrum. Mixing time: 0.5 s.

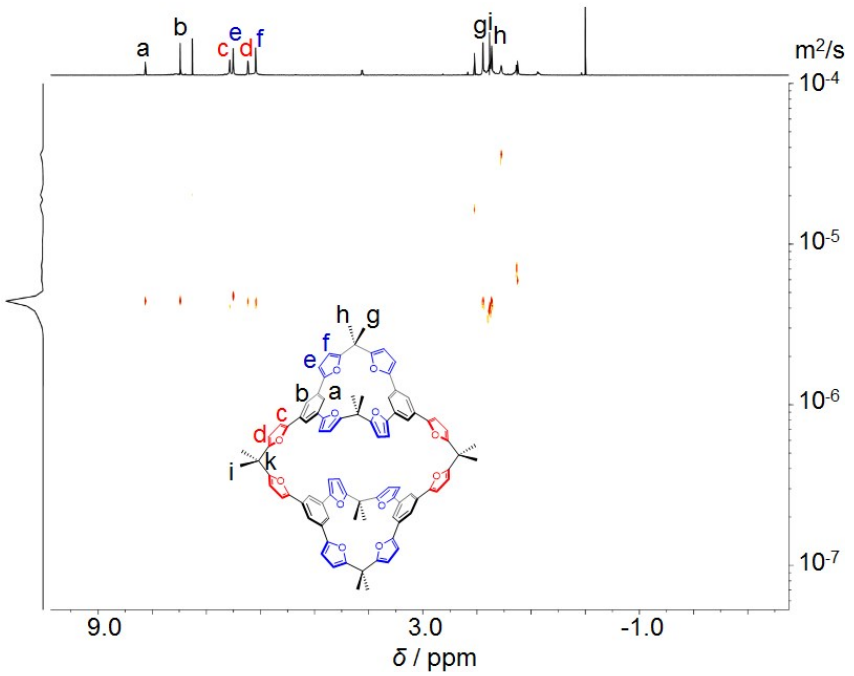

Figure S6. ^{1}H DOSY NMR spectrum of **1** ($CDCl_3$, 500 MHz, 298 K).

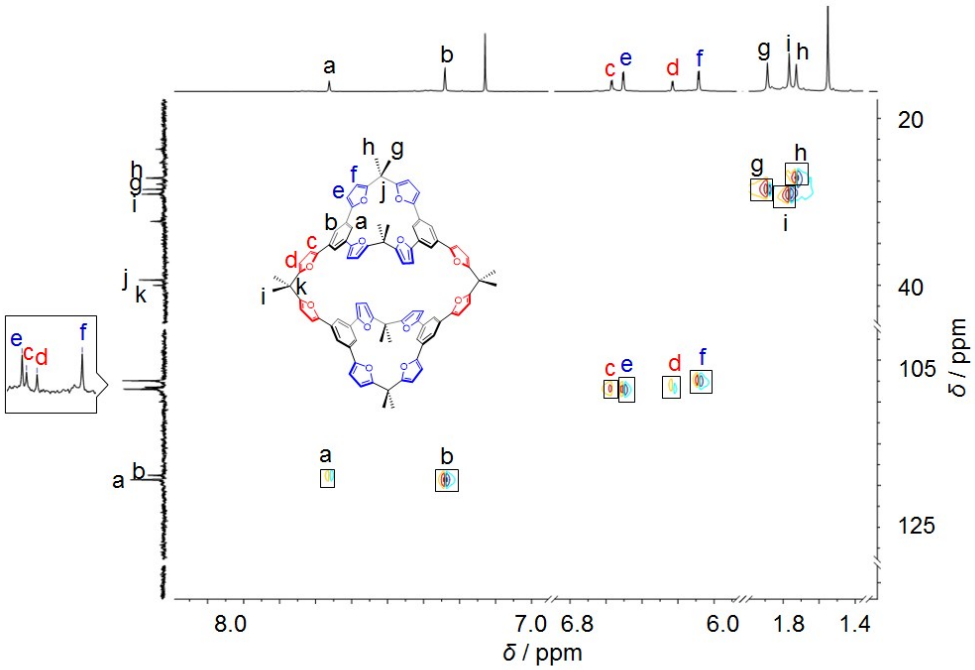

Figure S7. ^{1}H-^{13}C HSQC NMR spectrum of **1** ($CDCl_3$, 500 MHz, 298 K).

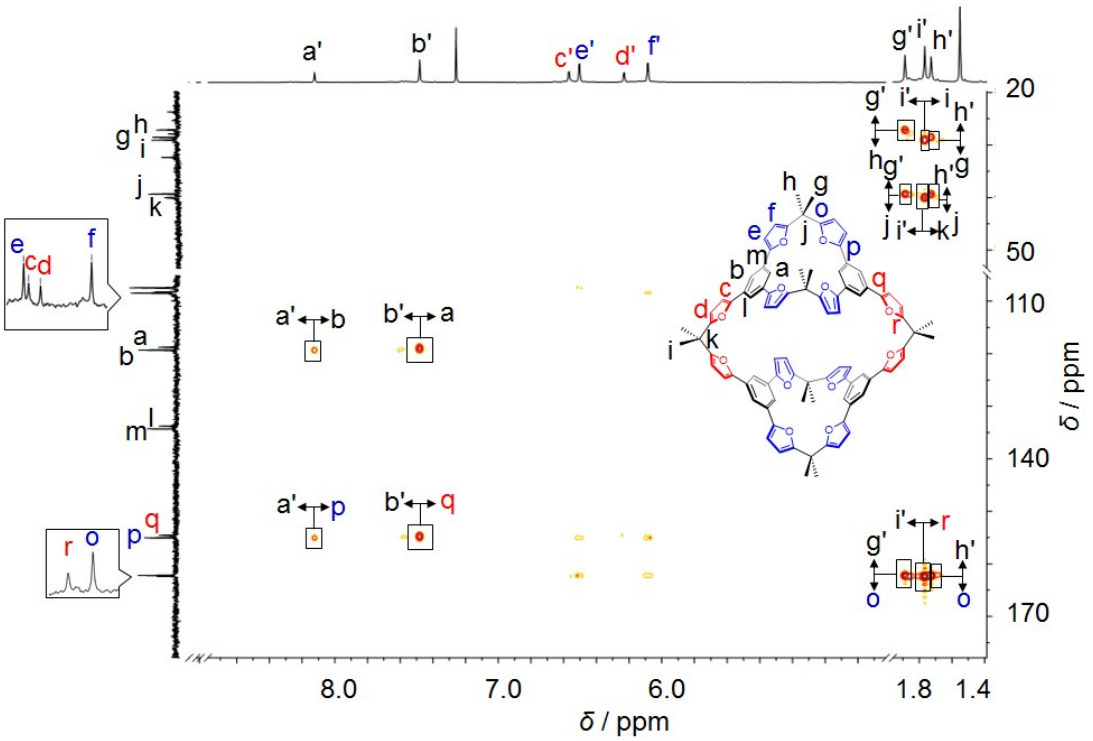

Figure S8. ^{1}H-^{13}C HMBC NMR spectrum of **1** ($CDCl_3$, 500 MHz, 298 K).

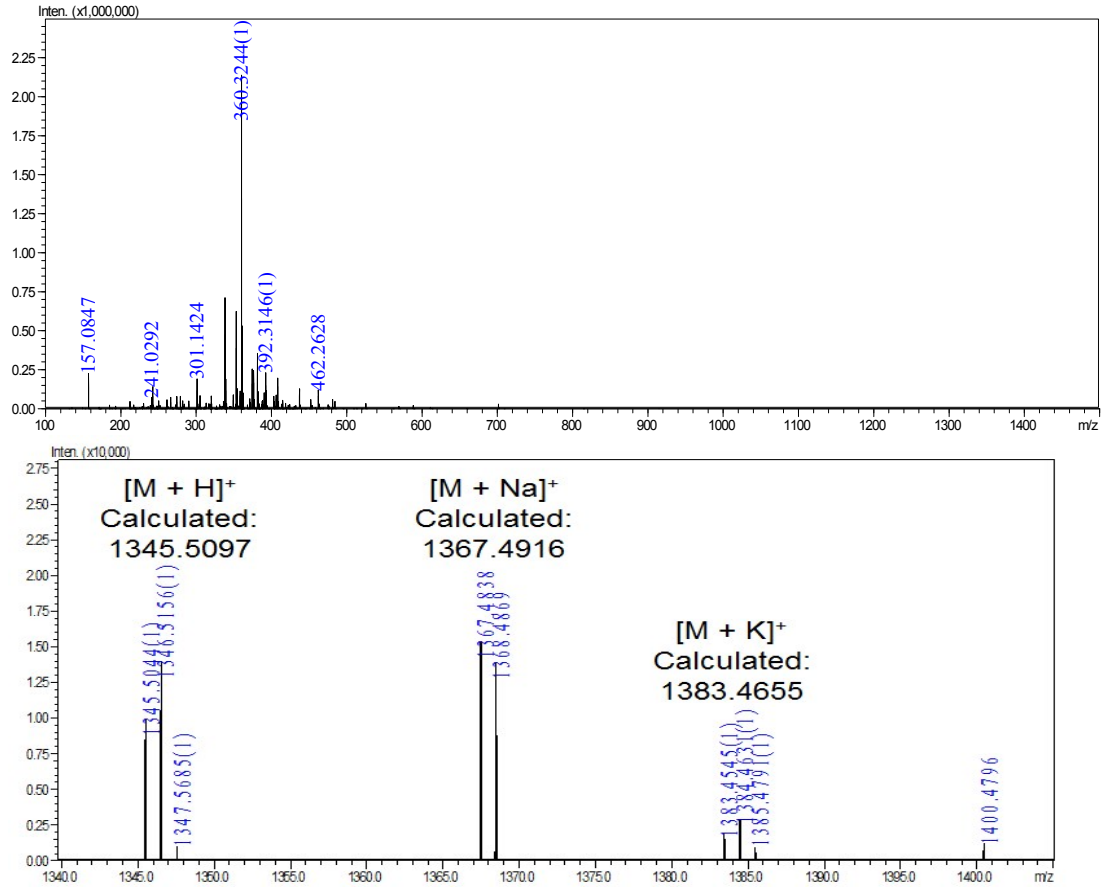

Figure S9. ESI-HRMS of **1**, full range (top), and expanded (bottom). Molecular ions bearing one positive charge by taking proton, sodium and potassium cations are observed.

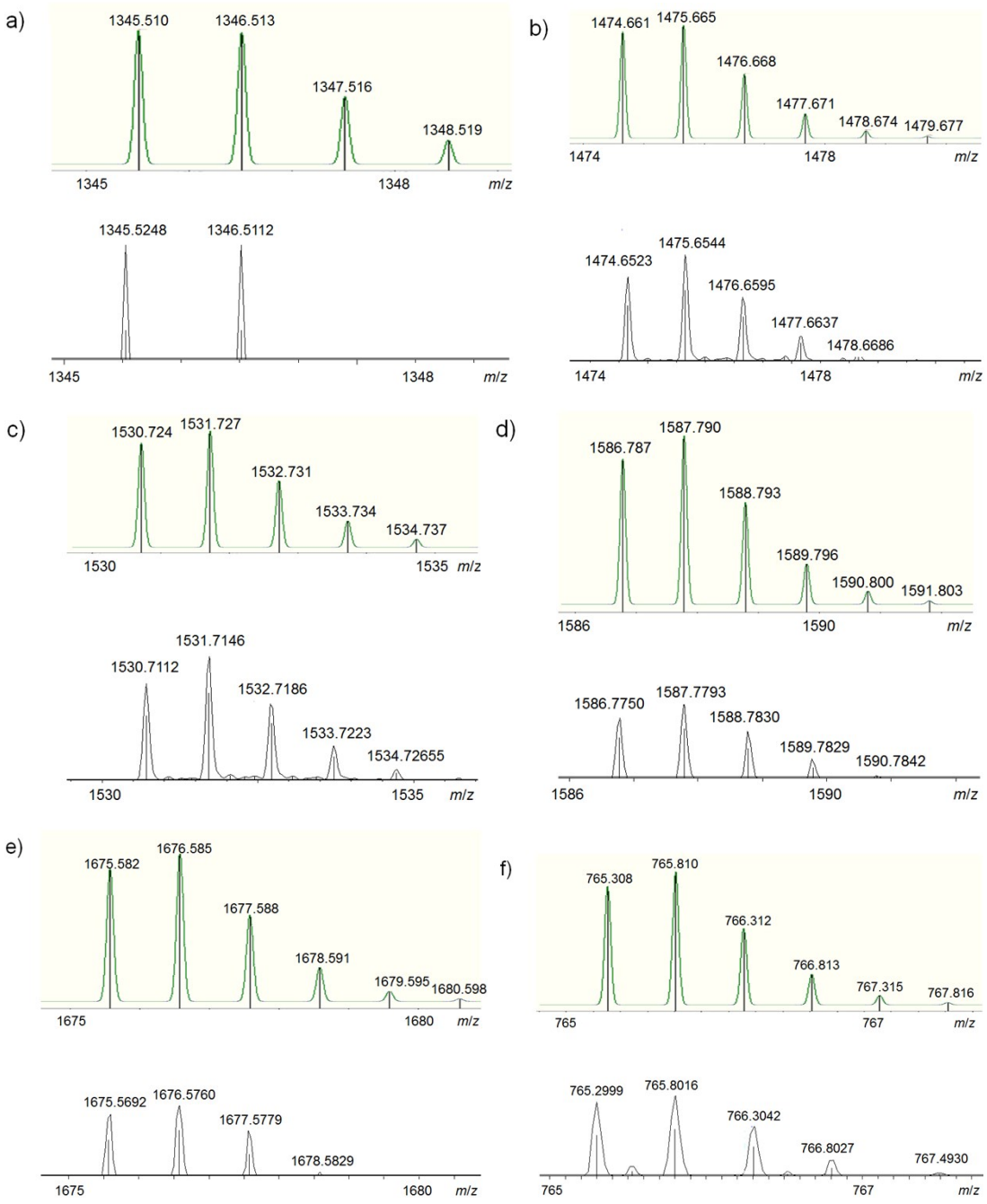

Figure S10. Experimental (bottom) and simulated(top) isotopic patterns of the peaks in ESI-HRMS, corresponding to a) [**M** + H]$^+$; b) [**M** + TEA]$^+$; c) [**M** + TPA]$^+$; d) [**M** + TBA]$^+$; e) [**M** + viologen]$^+$; f) [**M** + viologen + PF_6^-]$^+$. **M** is referred to as the macrocycle **1**.

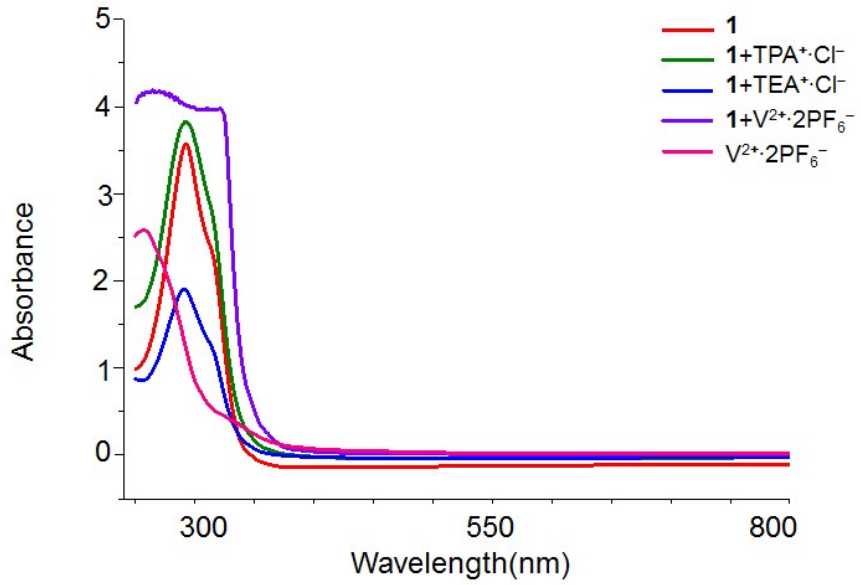

Figure S11. UV-Vis absorption spectrum of the macrocycle **1** in the absence and presence of guest. No charge-transfer bands in the visible light region were observed.

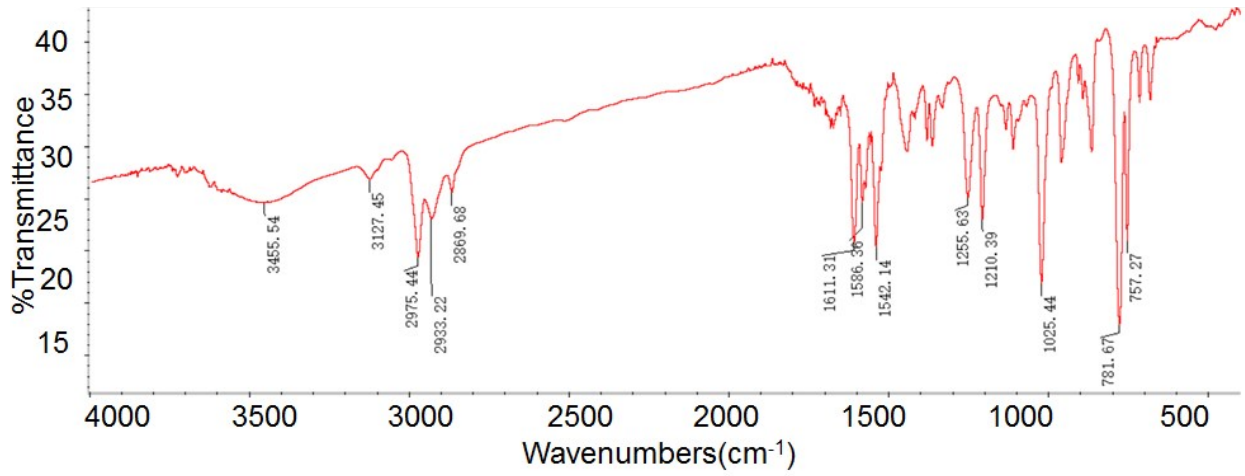

Figure S12. IR spectrum of **1**.

4. ^{1}H NMR titration

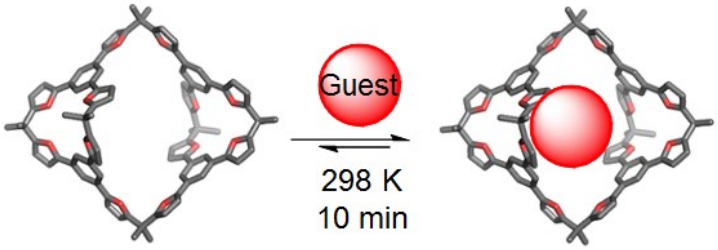

Fast Host-guest exchange on the NMR time scale was observed, as inferred from the results that before and after adding guests, only one set of peaks corresponding to the host and guests were observed. Binding affinities of the host-guest complexes were calculated by using ^{1}H NMR spectroscopic titration experiments. Solvent is either $CDCl_3$ for tetraalkylammonium chloride or 1:1 mixture of $CDCl_3$ and CD_3CN in the case of viologen whose counterion is PF_6^-. In all samples during titration, the concentration of the cage **1** was kept constant. The association constants (K_a) could be deprived from a plot of the resonance changes of a proton on the host cage **1** versus the concentration of the guest added into the solution of the cage **1**. K_a was calculated by using the plot to fit in the following equation[s2]:

$$A = ((1+1/K_a/[H]_0+[G]/[H]_0) - A_\infty((1+1/K_a/[H]_0+[G]/[H]_0)^2-4[G]/[H]_0)^{0.5})/2$$

Where A is the resonance changes of the aromatic proton on **1** host in the presence of the guest whose concentration is [G], A_∞ is the chemical shift change of H_e when the cavity of the host is completely occupied by the guest, and $[H]_0$ is the concentration of the host which was kept constant.

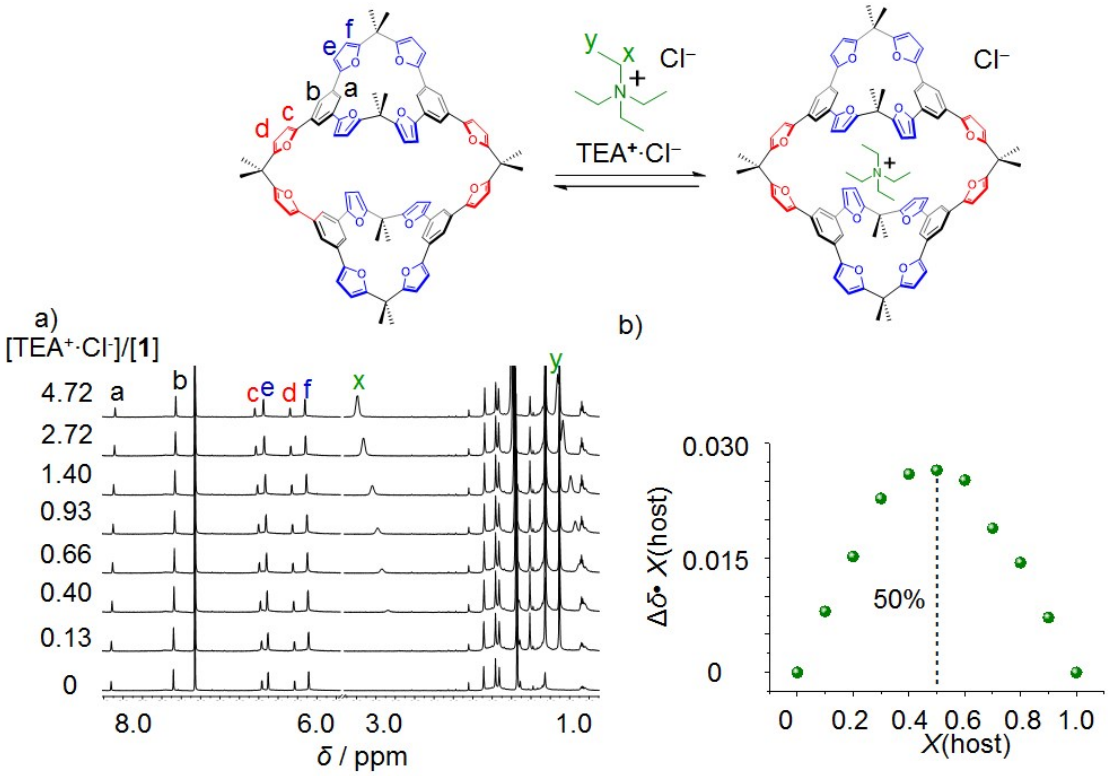

Figure S13. a) Partial ^{1}H NMR spectra ($CDCl_3$, 298K, 500 MHz) of **1** (1 mM) upon adding tetraethylammonium chloride ($TEA^+ \cdot Cl^-$) with different concentrations. b) A Job plot of $\Delta\delta \bullet X$(host) versus X(host). In all the ^{1}H NMR spectroscopic experiments for making Job plot, [**1**] + [$TEA^+ \cdot Cl^-$] = 1 mM, and the $\Delta\delta$ of the proton H_c was used to make the Job plot.

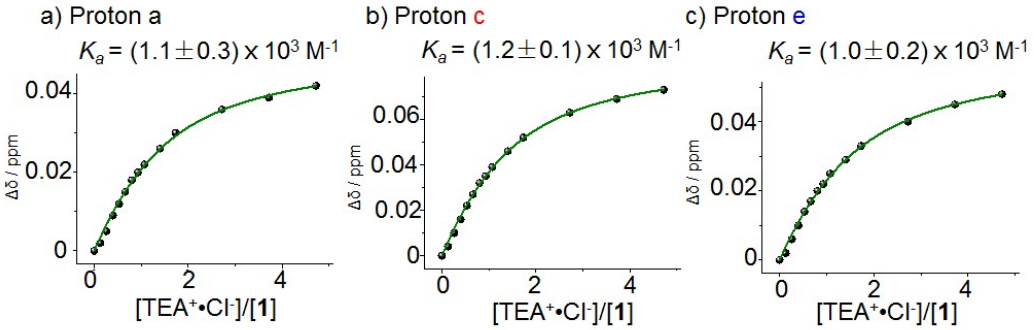

Figure S14. Plots of the upfield shifts of the resonance corresponding to protons H_a, H_c and H_e versus [$TEA^+ \cdot Cl^-$]/[**1**], respectively, based on ^{1}H NMR spectroscopic results in Figure S13a. K_a of **1** to recognize TPA^+ was calculated to be (1.1 in Fi x 10^3 M^{-1}, by averaging the three numbers.

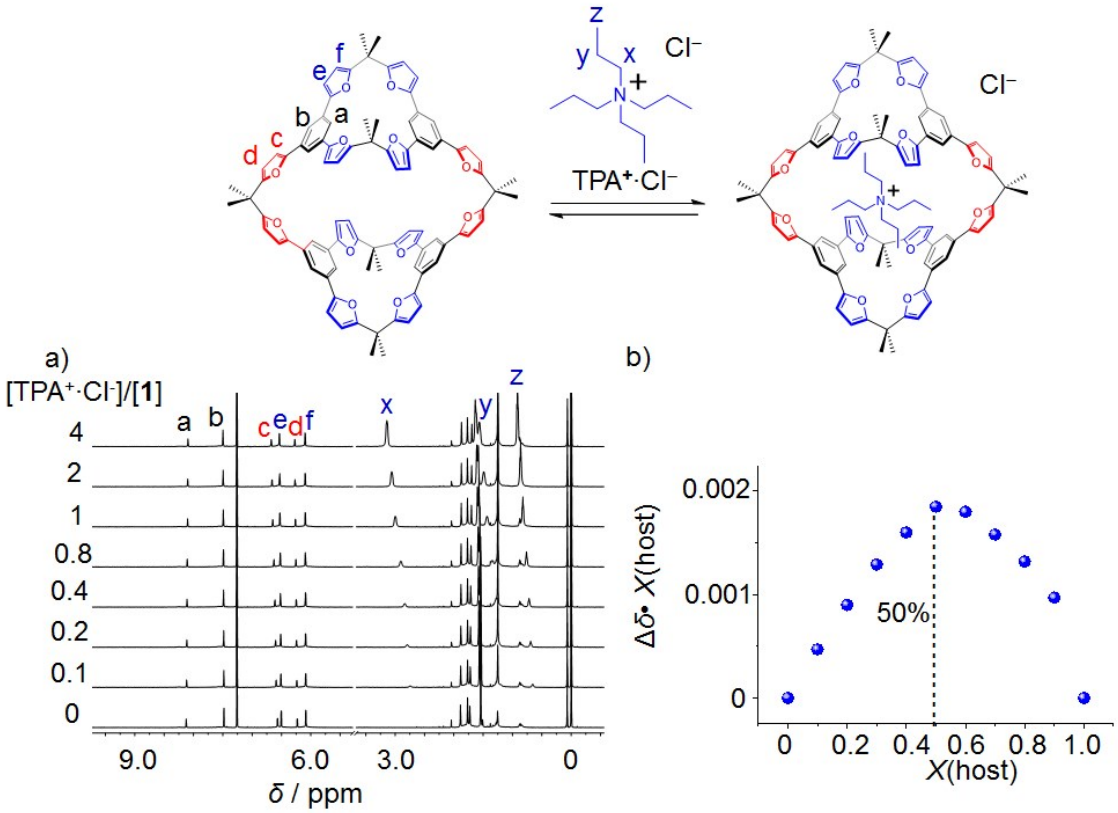

Figure S15. a) Partial ^{1}H NMR spectra ($CDCl_3$, 298K, 500 MHz) of **1** (1 mM) upon adding tetraethylammonium chloride ($TPA^+ \cdot Cl^-$) with different concentrations. b) A Job plot of $\Delta\delta \bullet X$(host) versus X(host). In all the ^{1}H NMR spectroscopic experiments for making Job plot, [**1**] + [$TPA^+ \cdot Cl^-$] = 1 mM, and the $\Delta\delta$ of the proton H_d was used to make the Job plot.

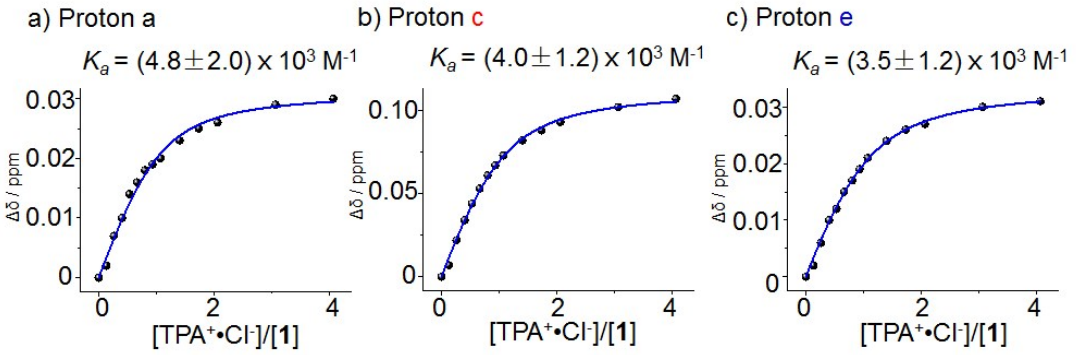

Figure S16. Plot of the upfield shifts of the resonance corresponding to protons H_a, H_c and H_e versus [$TPA^+ \cdot Cl^-$]/ [**1**], respectively, based on ^{1}H NMR spectroscopic results in Figure S15a. K_a of **1** to recognize TPA^+ was calculated to be (4.1 in Fi x 10^3 M^{-1}, by averaging the three numbers.

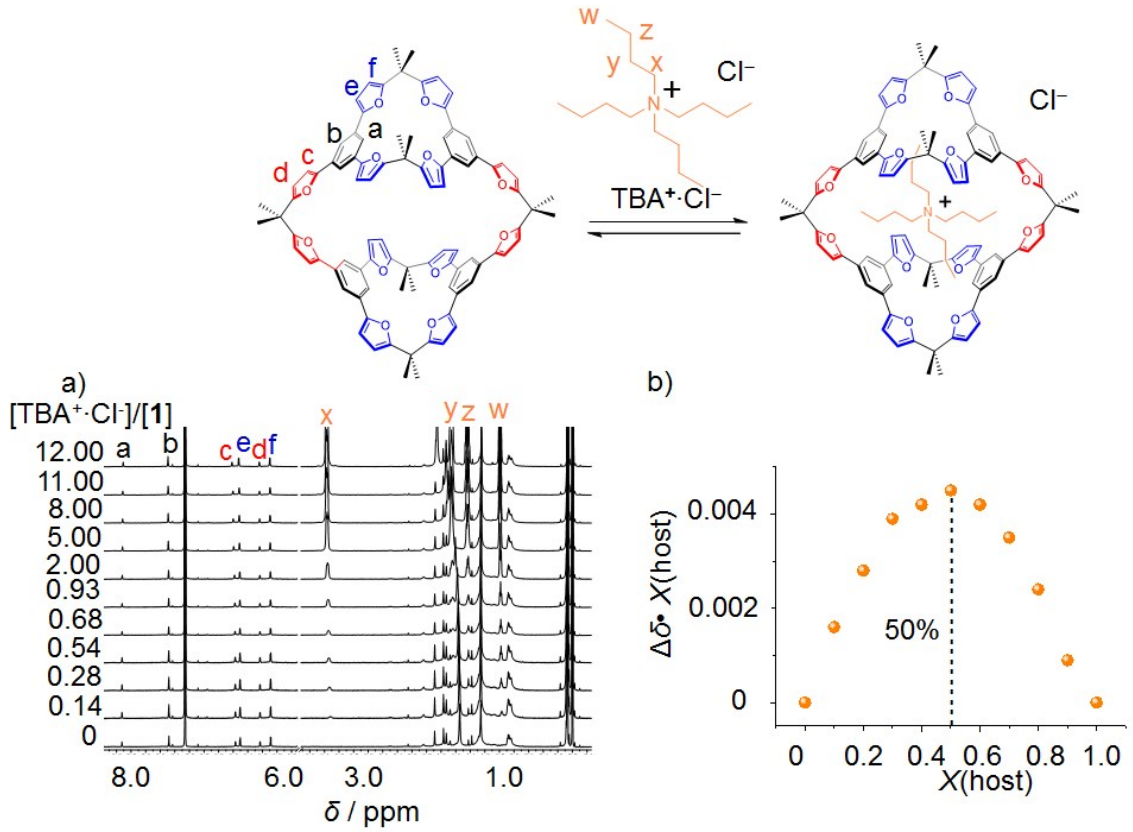

Figure S17. a) Partial ^{1}H NMR spectra ($CDCl_3$, 298K, 500 MHz) of **1** (1 mM) upon adding tetraethylammonium chloride ($TBA^+ \cdot Cl^-$) with different concentrations. b) A Job plot of $\Delta\delta \bullet X$(host) versus X(host). In all the ^{1}H NMR spectroscopic experiments for making Job plot, [**1**] + [$TBA^+ \cdot Cl^-$] = 1 mM, and the $\Delta\delta$ of the proton H_c was used to make the Job plot.

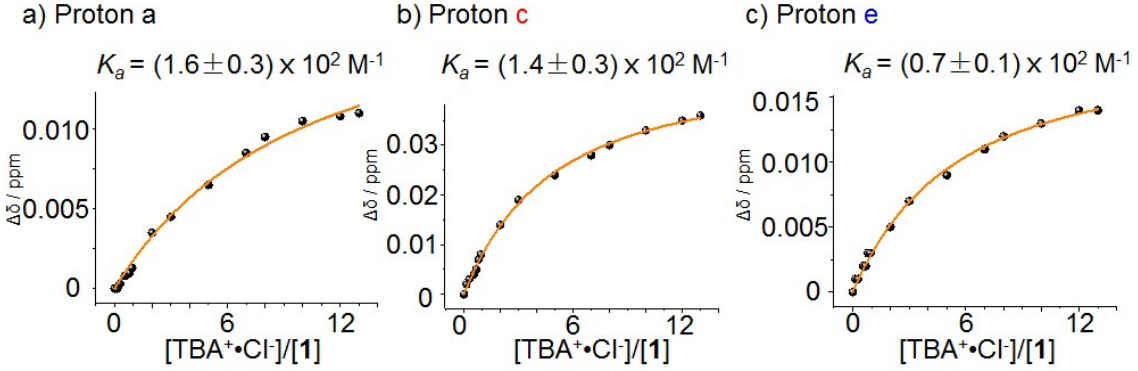

Figure S18. Plot of the upfield shifts of the resonance corresponding to protons H_a, H_c and H_e versus [$TBA^+ \cdot Cl^-$]/ [**1**], respectively, based on ^{1}H NMR spectroscopic results in Figure S17. K_a of **1** to recognize TBA^+ was calculated to be (1.2 ± 0.2) x 10^2 M^{-1}, by averaging the three numbers.

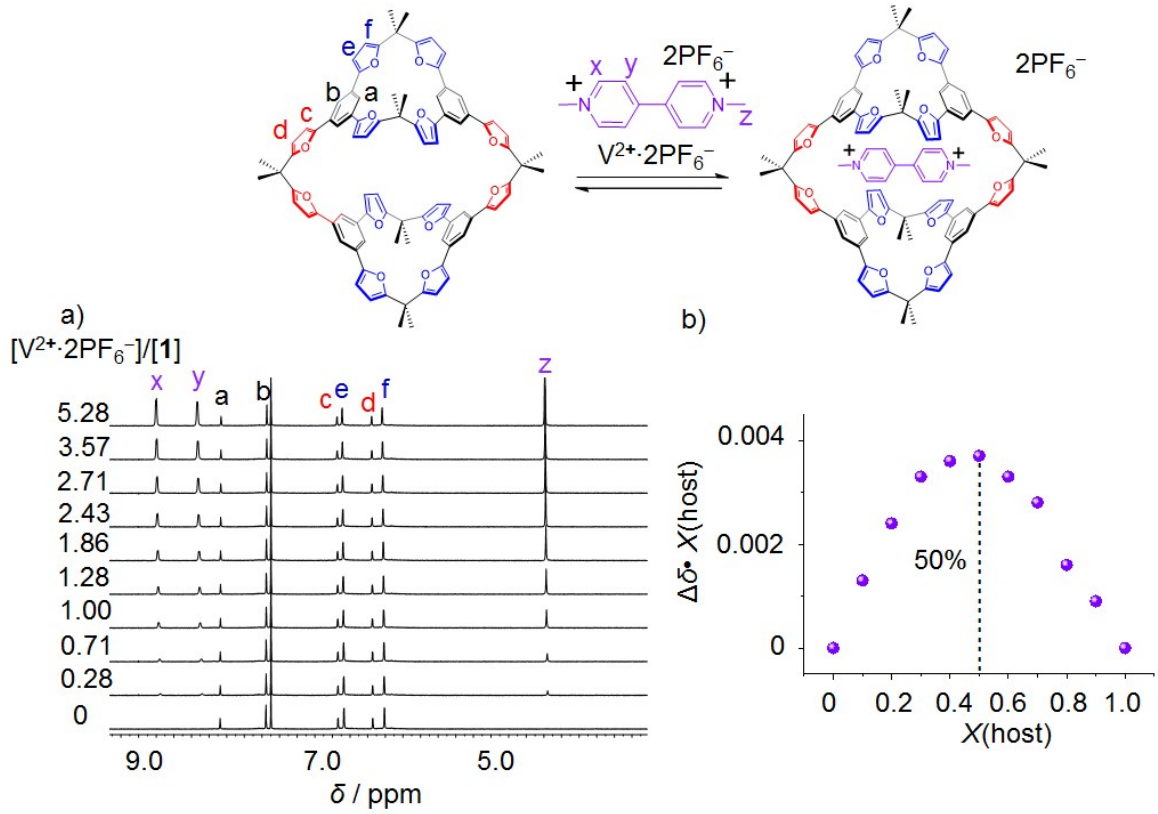

Figure S19. a) Partial ^{1}H NMR spectra ($CDCl_3$:CD_3CN = 1:1, 298K, 500 MHz) of **1** (1 mM) upon adding viologen whose counterion is PF_6^- with different concentrations. b) A Job plot of $\Delta\delta \bullet X$(host) versus X(host). In all the ^{1}H NMR spectroscopic experiments for making Job plot, [**1**] + [$V^{2+}\cdot PF_6^-$] = 1 mM, and the $\Delta\delta$ of the proton H_c was used to make the Job plot.

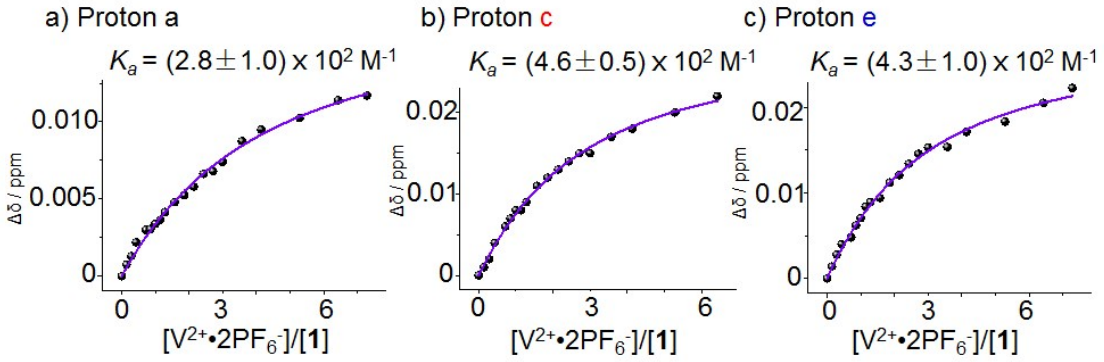

Figure S20. Plot of the upfield shifts of the resonance corresponding to protons H_a, H_c and H_e versus [viologen]/ [**1**], respectively, based on ^{1}H NMR spectroscopic results in Figure S19. K_a of **1** to recognize V^{2+} was calculated to be (3.9 in Fi x 10^2 M^{-1}, by averaging the three numbers.

5. Reaction monitoring

Method: 1,3,5-tri(furan-2-yl) benzene (TFB) (200 mg, 0.72 mmol) and acetone (0.239 mL, 3.26 mmol) were dissolved in anhydrous dichloromethane (48 mL). $SnCl_4$ (0.256 mL, 2.17 mmol) was added slowly. For a specific reaction time, we took 1 mL solution out from the reaction flask, and used water to quench the reaction. The mixture was then extracted with DCM. The organic layers were combined and then the organic solvent was removed under vacuum. The residue was dissolved in 0.5 mL $CDCl_3$ and the ^{1}H NMR spectrum was recored.

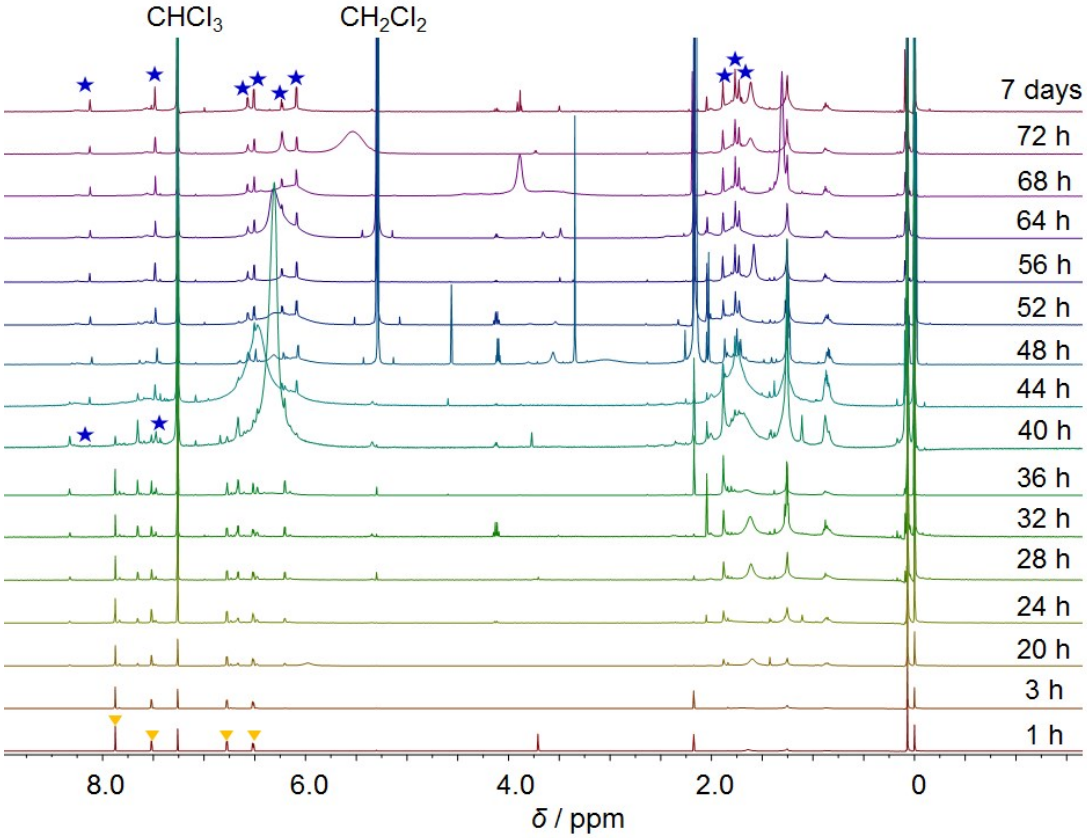

Figure S21. ^{1}H NMR spectra of the reaction mixture during the reaction course. The bule stars **(top)** correspond to the peaks of macrocycle **1**. The yellow triangles correspond to the peak of the reactant **TFB (bottom).**

The ^{1}H NMR spectra indicated that the reactant **TFB** was consumed after 40 h. After that, a set of sharp resonances were observed in the ^{1}H NMR spectra corresponding to the macrocycle **1**. The byproducts with substantial amount were not observable, because their resonances broaden out into the baseline. Between 32 h and 40 h, a set of tiny peaks were observed, which might correspond to half-macrocyle containing two or three TFB units.

6. Diels-Ader reactivity of 1

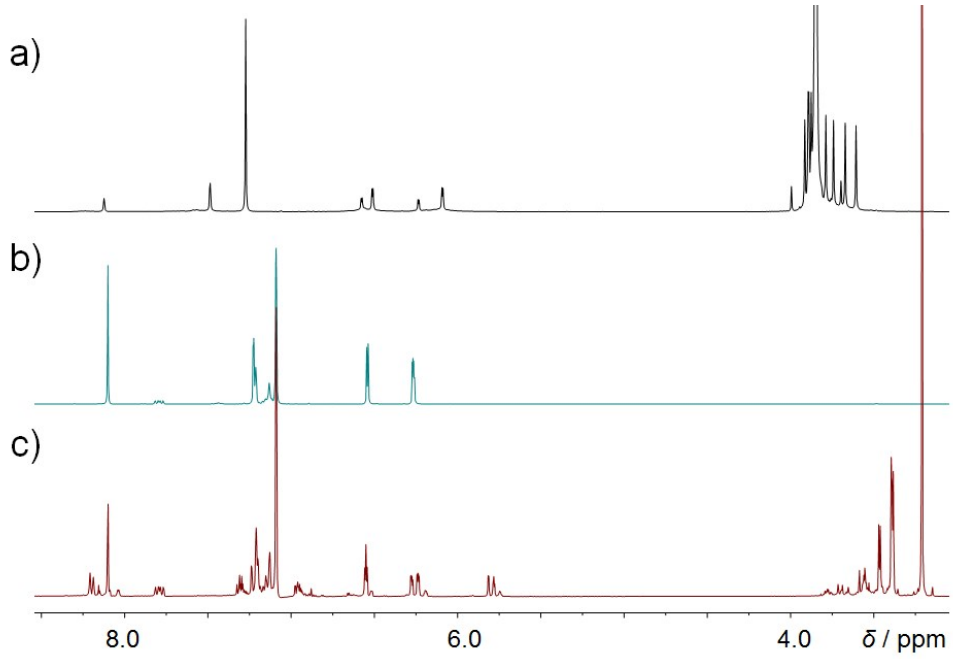

Figure S22. a) ^{1}H NMR spectrum of the mixture of **1** and dimethyl acetylenedicarboxylate after heating at 50 °C for 40h ($CDCl_3$, 500MHz). b) ^{1}H NMR spectrum of TFB (toluene-d_8, 500MHz). c) ^{1}H NMR spectrum of the mixture of **1** and dimethyl acetylenedicarboxylate after heating at 50 °C for 24h (toluene-d_8, 500MHz).

Diels-Alder reaction was observed (Figure S22 b, c) to occur by heating dimethyl acetylenedicarboxylate and 1,3,5-tri(furan-2-yl) benzene (TFB). As a comparison, such reaction did not occur (Figure S22 a) by heating **1** and dimethyl acetylenedicarboxylate after heating at 50 °C for 40h. We thus reasonably propose that the failure of the ring **1** in Diels-Alder reaction resulted from steric hindrance caused by the dimethyl bridges (the acetone residues).

7. X-ray crystallography

Methods

Single crystals of **1**, suitable for X-ray crystallography, were grown by slow vapor diffusion of diethyl ether into a solution of **1** in $CHCl_3$ after two weeks. Data were collected at 173 K on a Bruker D8 Venture Diffractometer equipped with a GaKα IμS source and MX optic.

Crystal parameters

$[C_{90}H_{72}O_{12}]$, colorless block (0.05 × 0.03 × 0.02 mm), triclinic, space group P -1, a = 11.934(8) Å, b = 12.680(8) Å, c = 15.587(11) Å, α = 83.19(2) °, β = 70.854(15) °, γ = 69.918(19) °, V = 2093(2) Å^3, Z = 1, T = 173 K, ρ_{calc} = 1.068 g/cm^3, μ(GaKα) = 1.34139 mm^{-1}. A total of 8284 reflections were collected, of which 2701 were unique. Final $R_1(I > 2\sigma(I))$ = 0.1412 and wR_2 = 0.4399 (all data). The structure was solved by direct method and different Fourier syntheses. Using Olex2, the structure was solved with the ShelXT structure solution program using Intrinsic Phasing and refined with the ShelXL refinement package using Least Squares minimization. The SQUEEZE procedure was done(see details in the cif file). The quality of the crystal is limited due to its easy collapse. CCDC number: 2058306.

Solid-state structure

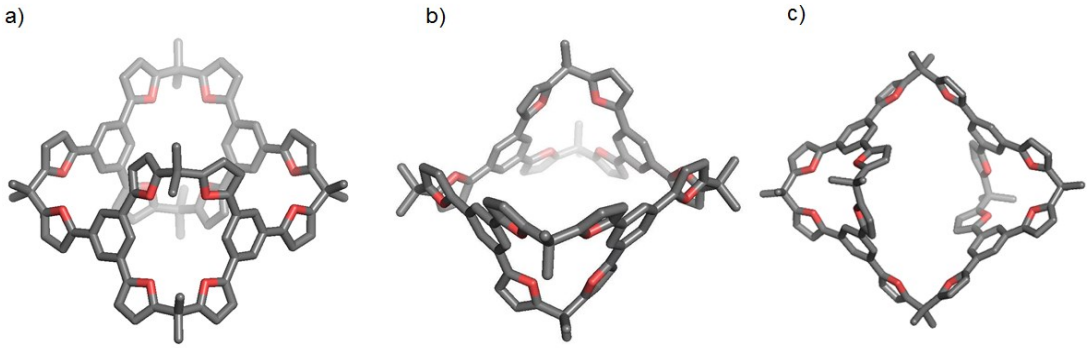

Figure S23. Different views of the solid-state structure of **1**. Color code: Carbon, grey; oxygen red; Disordered solvent molecules, and hydrogen atoms are omitted for clarity.

Cartesian Coordinates for 1

1	O1	7.8768	5.4973	2.4899
2	O2	5.2463	4.1311	2.2867
3	O3	2.6126	-1.8653	5.451
4	O4	7.465	-0.1609	1.577
5	O5	10.1402	1.2239	1.8936

6	O6	13.6967	3.8944	6.5774
7	C1	7.1108	6.5798	2.1351
8	C2	5.8668	6.2954	1.2825
9	C3	4.899	5.4364	2.1071
10	C4	4.2635	3.5466	3.0259
11	C5	3.302	4.4462	3.2777
12	H5	2.4923	4.2998	3.752
13	C6	3.7406	5.6594	2.6887
14	H6	3.2782	6.489	2.7119
15	C7	4.3728	2.098	3.3042
16	C8	3.5142	1.4858	4.1803
17	H8	2.877	2.0096	4.6512
18	C9	3.5629	0.1105	4.3953
19	C10	2.629	-0.4847	5.3155
20	C11	1.6479	-2.1785	6.3359
21	C12	1.0355	-1.044	6.7939
22	H12	0.3288	-0.9883	7.4261
23	C13	1.6749	0.0269	6.1283
24	H13	1.4709	0.949	6.234
25	C14	4.5372	-0.6158	3.7062
26	H14	4.597	-1.553	3.8484
27	C15	5.4029	-0.0286	2.8389
28	C16	6.3457	-0.8068	2.0511
29	C17	8.195	-1.0792	0.8467
30	C18	9.5172	-0.5646	0.3387
31	C19	10.3259	-0.084	1.5034
32	C20	10.8954	1.416	3.0082
33	C21	11.566	0.2856	3.341

34	H21	12.1811	0.1714	4.0562
35	C22	11.1595	-0.6841	2.4045
36	H22	11.419	-1.5979	2.3989
37	C23	10.8939	2.774	3.5957
38	C24	9.9236	3.6915	3.1452
39	H24	9.3132	3.4581	2.4547
40	C25	9.8819	4.9555	3.74
41	C26	8.9359	5.9517	3.2939
42	C27	8.8093	7.3066	3.4249
43	H27	9.382	7.8854	3.9136
44	C28	7.6509	7.6815	2.6857
45	H28	7.3147	8.5658	2.596
46	C29	10.7956	5.2969	4.7442
47	H29	10.7657	6.1665	5.1254
48	C30	11.7377	4.3924	5.1889
49	C31	12.6375	4.7379	6.2697
50	C32	14.4	4.4232	7.645
51	C33	15.6568	3.7212	8.0955
52	C34	16.7106	3.8304	6.9794
53	H34A	16.4115	3.3229	6.1966
54	H34B	17.5634	3.4662	7.2982
55	H34C	16.8297	4.7714	6.7332
56	C35	16.1897	4.3836	9.3751
57	H35A	16.9566	3.8751	9.711
58	H35B	15.4828	4.3957	10.0543
59	H35C	16.467	5.3017	9.1759
60	C36	13.7719	5.5522	8.0042
61	H36	14.0295	6.1206	8.7198

62	C37	12.6468	5.7655	7.1384
63	H37	12.0323	6.4891	7.1718
64	C38	11.7921	3.1164	4.5778
65	H38	12.4554	2.4928	4.8488
66	C39	10.2453	-1.7493	-0.3328
67	H39A	11.0706	-1.4296	-0.7529
68	H39B	9.6638	-2.1465	-1.0137
69	H39C	10.4637	-2.424	0.3443
70	C40	9.2885	0.6088	-0.6655
71	H40A	8.8336	1.3465	-0.2077
72	H40B	8.7349	0.297	-1.4118
73	H40C	10.1525	0.9196	-1.0073
74	C41	7.5061	-2.2381	0.8319
75	H41	7.7697	-3.031	0.3806
76	C42	6.3327	-2.0829	1.5976
77	H42	5.6676	-2.7401	1.7615
78	C43	5.3462	1.3815	2.6607
79	H43	5.9774	1.821	2.1032
80	C44	5.2005	7.6162	0.9365
81	H44A	4.85	8.0295	1.7525
82	H44B	4.4643	7.4552	0.3094
83	H44C	5.8567	8.2148	0.5224
84	C45	6.2459	5.5545	0.0177
85	H45A	6.8655	6.1014	-0.5083
86	H45B	5.4399	5.3742	-0.5087
87	H45C	6.6785	4.7066	0.2537
88	O1	9.1694	-5.3983	12.2346
89	O2	11.7999	-4.0322	12.4378

90	O3	14.4336	1.9642	9.2735
91	O4	9.5812	0.2598	13.1475
92	O5	6.906	-1.1249	12.8309
93	O6	3.3495	-3.7955	8.1471
94	C1	9.9354	-6.4809	12.5894
95	C2	11.1794	-6.1965	13.442
96	C3	12.1472	-5.3374	12.6174
97	C4	12.7827	-3.4477	11.6986
98	C5	13.7442	-4.3473	11.4468
99	H5	14.5539	-4.2009	10.9725
100	C6	13.3056	-5.5605	12.0358
101	H6	13.7679	-6.3901	12.0126
102	C7	12.6734	-1.999	11.4203
103	C8	13.532	-1.3868	10.5442
104	H8	14.1691	-1.9106	10.0733
105	C9	13.4833	-0.0116	10.3292
106	C10	14.4171	0.5837	9.4089
107	C11	15.3982	2.2774	8.3885
108	C12	16.0107	1.143	7.9306
109	H12	16.7173	1.0873	7.2984
110	C13	15.3712	0.0721	8.5962
111	H13	15.5753	-0.8501	8.4905
112	C14	12.5089	0.7147	11.0183
113	H14	12.4491	1.652	10.8761
114	C15	11.6433	0.1275	11.8856
115	C16	10.7004	0.9057	12.6734
116	C17	8.8511	1.1782	13.8778
117	C18	7.529	0.6635	14.3858

118	C19	6.7202	0.1829	13.2211
119	C20	6.1507	-1.317	11.7163
120	C21	5.4802	-0.1867	11.3835
121	H21	4.865	-0.0724	10.6683
122	C22	5.8867	0.783	12.32
123	H22	5.6271	1.6969	12.3256
124	C23	6.1523	-2.675	11.1288
125	C24	7.1226	-3.5926	11.5793
126	H24	7.733	-3.3592	12.2698
127	C25	7.1643	-4.8566	10.9845
128	C26	8.1103	-5.8527	11.4306
129	C27	8.2369	-7.2077	11.2996
130	H27	7.6641	-7.7864	10.8109
131	C28	9.3953	-7.5826	12.0387
132	H28	9.7315	-8.4668	12.1285
133	C29	6.2505	-5.1979	9.9803
134	H29	6.2805	-6.0676	9.599
135	C30	5.3085	-4.2935	9.5356
136	C31	4.4086	-4.6389	8.4548
137	C32	2.6461	-4.3243	7.0795
138	C33	1.3894	-3.6223	6.629
139	C34	0.3355	-3.7315	7.7451
140	H34A	0.6347	-3.2239	8.5279
141	H34B	-0.5173	-3.3672	7.4263
142	H34C	0.2164	-4.6724	7.9913
143	C35	0.8565	-4.2847	5.3494
144	H35A	0.0895	-3.7762	5.0135
145	H35B	1.5634	-4.2967	4.6702

146	H35C	0.5791	-5.2027	5.5486
147	C36	3.2743	-5.4533	6.7203
148	H36	3.0167	-6.0217	6.0047
149	C37	4.3994	-5.6666	7.5861
150	H37	5.0138	-6.3901	7.5527
151	C38	5.2541	-3.0175	10.1466
152	H38	4.5908	-2.3939	9.8757
153	C39	6.8008	1.8482	15.0573
154	H39A	5.9756	1.5285	15.4774
155	H39B	7.3823	2.2455	15.7382
156	H39C	6.5825	2.5229	14.3802
157	C40	7.7576	-0.5099	15.39
158	H40A	8.2125	-1.2475	14.9322
159	H40B	8.3113	-0.198	16.1363
160	H40C	6.8936	-0.8207	15.7318
161	C41	9.5401	2.337	13.8926
162	H41	9.2765	3.13	14.3439
163	C42	10.7135	2.1818	13.1269
164	H42	11.3786	2.8391	12.963
165	C43	11.7	-1.2825	12.0638
166	H43	11.0688	-1.7221	12.6212
167	C44	11.8457	-7.5173	13.788
168	H44A	12.1961	-7.9305	12.972
169	H44B	12.5818	-7.3563	14.4151
170	H44C	11.1894	-8.1159	14.2021
171	C45	10.8003	-5.4556	14.7068
172	H45A	10.1807	-6.0025	15.2328
173	H45B	11.6063	-5.2753	15.2332

174 H45C 10.3677-4.6077 14.4708

8. References.

[s1] Hazra, C., Gandhamsetty, N., Park, S. *et al.* Borane catalysed ring opening and closing cascades of furans leading to silicon functionalized synthetic intermediates. *Nat Commun*, **2016, 7,** 13431.
[s2] a) Hirose, K., Determination of Binding Constants. In *Analytical Methods in Supramolecular Chemistry*, **2006**; pp 17-54; b) R. P. Ashton,R. Ballardini, V. Balzani, M. Belohradsky, M. T. Gandolfi, D. Philp, L. Prodi, F. M. Raymo,M. V. Reddington, N. Spencer, J. F. Stoddart, M. Venturi, D. J. Williams, *J. Am. Chem. Soc.*,**1996**, *118*, 4931–4951; c) Y. Inoue, K. Yamamoto, T. Wada, S. Everitt, X.-M. Gao, Z.-J. Hou,L.-H. Tong, S.-K. Jiang, H.-M. Wu, *J. Chem. Soc., Perkin Trans. 2*, **1998**, 1807−1816.